Journal of Experimental Botany, Vol. 63, No. 1, pp. 275–292, 2012
doi:10.1093/jxb/err278 Advance Access publication 21 September, 2011
This paper is available online free of all access charges (see http://jxb.oxfordjournals.org/open_access.html for further details)

Journal of Experimental Botany
www.jxb.oxfordjournals.org

RESEARCH PAPER

Role of *ARABIDOPSIS A-FIFTEEN* in regulating leaf senescence involves response to reactive oxygen species and is dependent on *ETHYLENE INSENSITIVE2*

Guan-Hong Chen[1,2], Chia-Ping Liu[2], Shu-Chen Grace Chen[2] and Long-Chi Wang[2,*]

[1] Institute of Biochemistry and Molecular Biology, National Yang-Ming University, 11221 Taipei, Taiwan
[2] Institute of Plant and Microbial Biology, Academia Sinica, 11529 Taipei, Taiwan

* To whom correspondence should be addressed. E-mail: lwang@gate.sinica.edu.tw

Received 29 April 2011; Revised 3 August 2011; Accepted 5 August 2011

Abstract

Leaf senescence is a highly regulated developmental process that is coordinated by several factors. Many senescence-associated genes (*SAGs*) have been identified, but their roles during senescence remain unclear. A sweet potato (*Ipomoea batatas*) *SAG,* named *SPA15*, whose function was unknown, was identified previously. To understand the role of *SPA15* in leaf senescence further, the orthologue of *SPA15* in *Arabidopsis thaliana* was identified and characterized, and it was named *ARABIDOPSIS A-FIFTEEN* (*AAF*). *AAF* was expressed in early senescent leaves and in tissues with highly proliferative activities. AAF was localized to the chloroplasts by transient expression in *Arabidopsis* mesophyll protoplasts. Overexpression of *AAF* (*AAF-OX*) in *Arabidopsis* promoted, but the T-DNA insertion mutant (*aaf-KO*), delayed age-dependent leaf senescence. Furthermore, stress-induced leaf senescence caused by continuous darkness was enhanced in *AAF-OX* but suppressed in *aaf-KO*. Transcriptome analysis of expression profiles revealed up-regulated genes related to pathogen defence, senescence, and oxidative stress in 3-week-old *AAF-OX* plants. Indeed, elevated levels of reactive oxygen species (ROS) and enhanced sensitivity to oxidative and dark stress were apparent in *AAF-OX* but reduced in *aaf-KO*. *ETHYLENE INSENSITIVE2* (*EIN2*) was required for the dark- and ROS-induced senescence phenotypes in *AAF-OX* and the induction of *AAF* expression by treatment with the immediate precursor of ethylene, 1-aminocyclopropane-1-carboxylic acid. The results indicate the functional role of *AAF* is an involvement in redox homeostasis to regulate leaf senescence mediated by age and stress factors during *Arabidopsis* development.

Key words: *Arabidopsis thaliana*, chloroplast, ethylene, leaf senescence, oxidative stress, reactive oxygen species, senescence-associated gene (*SAG*).

Introduction

Leaf senescence is a complex and highly regulated process in the final stage of plant development. One of the visible symptoms of senescence is leaf yellowing because of loss of chlorophyll (Smart, 1994). Environmental stresses, including heat, cold, drought, shedding, pathogen infection, and irradiation, induce leaf senescence (Lim *et al.*, 2007). In addition, the regulation of leaf senescence by developmental signals mainly depends on phytohormones and age (reviewed in Buchanan-Wollaston, 1997; Lim *et al.*, 2007). A number of senescence-associated genes (*SAGs*) have been identified to study the regulatory mechanism of leaf senescence (He *et al.*, 2001; Buchanan-Wollaston *et al.*, 2003; Gepstein *et al.*, 2003). However, the physiological role of many *SAGs* has yet to be defined.

Free radicals are proposed to play an essential role in leaf senescence (Strother, 1988). Reactive oxygen species (ROS) are toxic by-products of aerobic metabolism and include singlet oxygen ($^1O_2$), superoxide radical ($O_2^{\cdot -}$), hydroperoxyl radical ($HO_2^{\cdot -}$), hydrogen peroxide (H_2O_2), and hydroxyl radical ($OH^{\cdot}$). Many biological activities in plants lead to

accumulation of ROS (reviewed in Mittler *et al.*, 2004; Foyer and Noctor, 2009). Several biotic and abiotic stresses induce abrupt elevated ROS levels in plant cells. The hypersensitive response is a well-documented example of the rapid accumulation of H_2O_2 (oxidative burst) leading to cell death to prevent the spread of pathogens (Lamb and Dixon, 1997). The elevated level of H_2O_2 acts as the signal molecule eliciting plant responses to various stresses (Orozco-Cardenas *et al.*, 2001). Therefore, ROS are destructive by-products and also play a role in the activation of gene expression in response to pathogens and various abiotic stresses (Miller *et al.*, 2008, 2010). However, the mechanistic role of ROS in modulating leaf senescence remains unknown.

Plants react to oxidative stress by activating a series of antioxidative enzymes such as catalases, superoxide dismutases (SODs), and components of the ascorbate–glutathione cycle to maintain cellular redox homeostasis (Mittler, 2002). Perturbation of these antioxidants results in oxidative damage that may lead to cell death. Excessive ROS are present in chloroplasts of ageing plants (Munné and Alegre, 2002). The coordinated increase in membrane permeability, lipid peroxidation, and reduced activities of SODs and catalases occurs during leaf senescence (Dhindsa *et al.*, 1981). The connection between oxidative stress and leaf senescence is further supported by observations of the induction of several representative SAGs in response to oxidative stress (Miller *et al.*, 1999; John *et al.*, 2001; Navabpour *et al.*, 2003) and mutants showing delayed leaf senescence, such as *ore1*, *ore3*/*ein2*, and *ore9*, being more resistant to oxidative stress (Woo *et al.*, 2004; Cao *et al.*, 2006). Therefore, disruption of cellular redox homeostasis can lead to leaf senescence in plants. Only a few reports have described the regulatory role of ROS homeostasis in leaf senescence. *Arabidopsis cpr5*/*old1* shows accelerated leaf senescence during vegetative stages by induction of stress response leading to cell death due to a perturbed redox balance (Jing *et al.*, 2008). *Arabidopsis XDH1* encodes xanthine dehydrogenase involved in purine catabolism, and the *xdh1* mutant showed premature senescence symptoms, elevated ROS levels, and a higher mortality rate than the wild type when stressed plants recovered from dark treatment (Brychkova *et al.*, 2008).

A *SAG* was previously identified in sweet potato (*Ipomoea batatas*) by a differential display approach and it was named *SWEET POTATO A15* (*SPA15*) (Yap *et al.*, 2003). However, the physiological function of *SPA15* was not clear. Here the characterization of a *SPA15* orthologue in *Arabidopsis thaliana*, named *ARABIDOPSIS A FIFTEEN* (*AAF*), is reported. AAF has a predicted chloroplast transit peptide and was shown to be a plastid protein by transient expression assay in *Arabidopsis* mesophyll protoplasts. Overexpression of *AAF* resulted in an elevated level of cellular ROS, enhanced sensitivity to oxidative stress, and promoted leaf senescence induced by continuous darkness and by age-dependent signalling in plants. In addition, T-DNA insertion mutants of *AAF* were more resistant to oxidative stress and showed delayed leaf senescence mediated by developmental signalling or induced by darkness. Finally, it was shown that leaf senescence regulated by *AAF* depended on a functional *EIN2*. The results support *AAF* as a novel component involved in modulation of redox homeostasis that responds to developmental and stress-induced signals to regulate leaf senescence.

Materials and methods

Materials and plant growth conditions

All of the transgenic lines and mutants in this study were derived from the wild-type *A. thaliana* Columbia (Col-0) ecotype and cultivated in growth chambers under long days (LDs; 16 h light/8 h dark) or short days (SDs; 12 h light/12 h dark) at 22 °C under fluorescence illumination (100–150 μE m^{-2} s^{-1}). Seeds were sterilized by 10% bleach for 20 min, and then rinsed with distilled water. The sterilized seeds were stratified in the dark at 4 °C for 3 d and germinated on half-strength Murashige and Skoog (0.5× MS) medium (pH 5.7) supplemented with 1% sucrose and 0.8% (w/v) agar. Two T-DNA insertion mutants of *AAF* (At1g66330) were obtained from the Arabidopsis Biological Resource Center (WiscDsLox453-456F9 and GABI-Kat 762H05) and homozygosity was verified by genotyping with gene-specific primers (Supplementary Table S2 available at *JXB* online). To generate *AAF-OX*/*ein2-5*, *ein2-5* was crossed to *AAF-OX* (*AAF* overexpression), and F_2 plants were scored for ethylene insensitivity to identify homozygous *ein2-5* followed by genotyping of *35S::AAF*. For rapid PCR screening of mutants and transgenic plants, genomic DNA was extracted for analysis as described (Murray and Thompson, 1980).

Flowering time was scored by days after germination until the inflorescence reached 1 cm in height. The length of primary roots and density of root hairs of 5-day-old seedlings were measured and analysed by National Institutes of Health ImageJ software (http://imagej.nih.gov/ij/). For dark treatment, 3-week-old plants or detached leaves were incubated in a dark controlled environment (70% relative humidity at 22 °C) until samples were collected at the indicated times. For hormone treatments, 7-day-old light-grown seedlings were transferred to 0.5× MS liquid medium for 24 h before addition of various hormones, and samples were collected at the indicated times for extraction of total RNA. 1-Aminocyclopropane-1-carboxylic acid (ACC) was purchased from Calbiochem (Merck), and other chemicals, including abscisic acid (ABA), methyl jasmonate (MeJA), and salicylic acid (SA), were from Sigma, unless otherwise indicated.

Plasmid construction and plant transformation

To generate the overexpression construct of *AAF* under the control of a *Cauliflower mosaic virus* (CaMV) *35S* promoter, the full-length coding sequence of *AAF* was amplified by PCR with the primers ATA15SpeIF1 and ATA15PmlIR2, and digested by *Spe*I and *Pml*I. The *Spe*I/*Pml*I fragment was subcloned into *Spe*I and *Pml*I sites of pCAMBIA1302z for *35S::AAF*. To construct the promoter fusion of *AAF* with β-glucuronidase (*GUS*) for analysis of tissue-specific expression profiles, a DNA fragment containing 2020 bp from 5′ upstream of *AAF* including 220 bp of 5′-untranslated region (UTR) was amplified by PCR with the primers ATA15-GFP-f1 and ATA15-GFP-r1, and digested with *Eco*RI and *Bam*HI. The *Eco*RI/*Bam*HI fragment was subcloned to pCAMBIA1391z Xb for *AAFpro::GUS*. These constructs were introduced into the *Agrobacterium tumefaciens* strain LBA4404 or GV3101 for subsequent transformation to *Arabidopsis* by the floral-dip method (Clough and Bent, 1998). Transgenic plants were selected by hygromycin (25 μg ml^{-1}) resistance and propagated to homozygous lines. The coding sequence of *AAF* or *SPA15* was amplified by PCR with the following primers: ATA15F8 and ATA15R9 for full-length cDNA of *AAF* (1–417); ATA15-41F and ATA15R9 for $AAF_{41–417}$; ATA15FL-attB1F and ATA1540-attB2R for $AAF_{1–41}$; and SPA15-attB1F and SPA15-attB1R for the full-length cDNA of

SPA15 (1–426). The Gateway system (Invitrogen) was used to generate various *AAF* and *SPA15* constructs for use in the transient expression assay with *Arabidopsis* mesophyll protoplasts. The DNA fragments were subcloned to pCR8/GW/TOPO or pDONR221 by BP reactions as the entry clones, which were subsequently cloned to a pPZP-based destination vector by LR reactions for the three *35S::AAF–GFP* (green fluorescent protein) constructs used in Fig. 2. All of the primers described above are listed in Supplementary Table S2 at *JXB* online.

β-Glucuronidase assay and protoplast transient assay for protein localization

Seedlings and plant organs collected at different developmental stages were incubated with 0.5 mg ml^{-1} 5-bromo-4-chloro-indolyl-β-D-glucuronide (X-Glu) in 100 mM phosphate buffer (pH 7.0) at 37 °C overnight. Chlorophyll was removed from leaves by clarification with 70% ethanol before observation. Preparation of *Arabidopsis* mesophyll protoplasts and subsequent transfection by polyethylene glycol (PEG)-4000 for transient expression assay were performed as described (Sheen, 2001). Fluorescence images of GFP fusions were acquired by confocal laser scanning microscopy (Zeiss LSM 510 Meta).

Assays for age- and dark-induced leaf senescence

For age-dependent leaf senescence, the third and fourth rosette leaves of individual plants were used for analyses of chlorophyll content, photochemical efficiency, and membrane ion leakage. Leaves were collected and incubated in 96% (v/v) ethanol (3 mg of tissue in 1 ml of ethanol) at room temperature in the dark for 30 min. After centrifugation, the supernatant was used for quantification of chlorophyll levels by spectrophotometry (U-2001, Hitachi) as described (Wintermans and de Mots, 1965). The photochemical efficiency of photosystem II (PSII) activity was measured by a hand-held chlorophyll fluorimeter (Pocket PEA, Hansatech Instruments). Membrane ion leakage was analysed by electrolytes released from leaves by using a bench-top conductivity meter (CON500, CLEAN Instruments). Four leaf discs were removed from designated leaves of experimental plants, and the third and fourth leaves were used in the age-dependent senescence assay in Fig. 3 and the fifth and sixth leaves in the dark-induced senescence assay in Fig. 5. These discs were thoroughly washed by deionized water three times, followed by immersion in 25 ml of 400 mM mannitol at 22 °C for 3 h with gentle shaking before measuring the initial conductivity. Total conductivity was measured after five freeze–thaw cycles using liquid nitrogen and a water bath set at 25 °C for maximum membrane disruption. The conductivity resulting from membrane ion leakage is presented as the percentage of initial conductivity versus total conductivity. These experiments were repeated three times with consistent results, and a representative set of data is shown with standard errors. For dark-induced leaf senescence, the fifth and sixth leaves of 4-week-old plants were collected and incubated in 3 mM MES buffer (pH 5.8) for continuous darkness treatment for 5 d. Analyses for leaf senescence by measuring chlorophyll levels, photochemical activity, and membrane ion leakage were performed as described above.

Electron microscopy

The fifth or sixth leaves of 3-week-old plants were fixed in 2.5% glutaraldehyde and 4% paraformaldehyde in 0.1 M sodium phosphate buffer, pH 7.0, at room temperature for 4 h. After three 20 min rinses, the samples were fixed in 1% OsO_4 in the same buffer for 4 h, then rinsed three times with buffer. Samples were dehydrated in an acetone series, embedded in Spurr's resin, and sectioned with use of a Leica Reichert Ultracut S or Leica EM UC6 ultramicrotome (Leica Microsystems GmbH). The ultrathin sections (70–90 nm) were stained with uranyl acetate and lead citrate. A Philips CM 100 TEM (FEI Company) at 80 kV was used for viewing.

Chemical treatments with oxidative stress-inducing agents and analysis of cellular levels of ROS

All the experiments on detached leaves were performed with the fifth and sixth rosette leaves of 3-week-old plants (counting from the true leaves). Detached leaves were incubated in 3 mM MES buffer (pH 5.8) in the presence of oxidative stress-inducing reagents, H_2O_2 and paraquat, then treated leaves were ground in liquid nitrogen, and the chlorophyll content was determined by spectrophotometry.

To visualize H_2O_2 *in situ*, DAB (3,3′-diaminobenzidine) was infiltrated into detached leaves and stained leaves as described (Rea *et al.*, 2004). For the detection of ROS by fluorescence, 7-day-old seedlings were transferred to 0.5× MS liquid medium with 50 μM 2′,7′-dichlorofluorescein diacetate (DCFDA; Invitrogen) for 30 min in the dark. After being briefly washed with distilled water, the roots were examined for fluorescence by confocal laser scanning microscopy (Zeiss LSM 510 Meta) with excitation at 488 nm and emission at 500–530 nm.

Quantification of H_2O_2 and MDA

The Amplex Red Hydrogen Peroxide/Peroxidase Assay kit (Molecular Probes) was used to quantitate H_2O_2 levels. Plant leaves were ground to powder with liquid nitrogen, and 30 mg of tissues were mixed with 200 μl of phosphate buffer (20 mM K_2HPO_4, pH 6.5). After centrifugation, 50 μl of the supernatant was incubated with 50 μl of working solution consisting of 100 μM Amplex Red reagent and 0.2 U ml^{-1} horseradish peroxidase at room temperature for 30 min under dark conditions. The fluorescence was quantified by use of a plate reader (Plate CHAMELEON, Hidex Oy) with excitation at 545 nm and emission at 580 nm.

For quantification of MDA, 100 mg of leaf tissue was ground to powder with liquid nitrogen and extracted by 1 ml of 20 mM phosphate buffer (pH 7.4). Butylated hydroxytoluene (10 μl, 0.5 M) in acetonitrile was added to 1 ml of tissue homogenate to prevent sample oxidation, and 200 μl of supernatant was used for assay after centrifugation. A colorimetric assay for lipid peroxidation was used to quantitate MDA levels following the manufacturer's protocol (Oxford Biomedical Research).

Microarray experiments, statistical analysis and RT-PCR

Microarray experiments were performed by use of an Arabidopsis ATH1 GeneChip (Affymetrix). Rosette leaves of 3-week-old plants were used to prepare RNA samples. At this stage, no senescent phenotype was visible. RNA preparation, labelling, and hybridization followed the instructions of an in-house core facility (http://ipmb.sinica.edu.tw/affy/). Data from two independent biological replicates were imported to Genespring GX10 software and analysed by the RMA method. Genes were selected by at least a 1.5-fold change of signals compared with the wild type and if present in two biological replicates. The distribution of Gene Ontology (GO) annotations of genes up-regulated in *AAF-OX* was processed by the web-based program at TAIR (http://www.arabidopsis.org). GO-specific terms were investigated by use of AmiGO (http://amigo.geneontology.org) and the GO database released in October 2009 (Ashburner *et al.*, 2000). *P*-values were calculated by Fisher's test (http://www.langsrud.com/fisher.htm) (Agresti, 1992). Statistical analysis involved Student's *t*-test. A significant difference between the control and experimental groups was considered with $P < 0.05$.

Total RNA was extracted by TRIzol reagent, and reverse transcription was performed by using 1 μg of RNA at 50 °C by MMLV (TOYOBO) reverse transcriptase according to the manufacturer's protocol. RT-PCR was performed with gene-specific primers (Supplementary Table S2 at *JXB* online). Real-time PCR

analyses were performed with a qPCR machine (MX3000P, Stratagene) in a volume of 20 µl, including qPCR master mix (Kapa Biosystems), 0.2 µM of gene-specific primers (Supplementary Table S3), and 50 nM ROX™ as a passive reference dye for factor calibration. Data were normalized to the expression of *ACTIN2* (At3g46520).

Results

Expression patterns of AAF *in* Arabidopsis

SPA15 was classified as a *SAG* isolated from senescent leaves of sweet potato with unknown functions (Huang *et al.*, 2001). The expression of *SPA15* and its orthologue in rice was induced in senescing leaves, which suggests a physiological role for *SPA15* in leaf senescence. To study further the function of *SPA15* in a reference plant, *AAF* was identified as the *A. thaliana* orthologue of *SPA15*. AAF is encoded by a single locus based on the latest release of the Arabidopsis genome database (TAIR10). *AAF* is a plant-specific gene present in both monocots and dicots, and encodes a novel protein without any defined domain of known function. Protein alignment revealed that two-thirds of the C-terminal region of AAF (amino acids 118–417) was highly conserved in orthologues from different species with sequence identity >70%, except for the moss (50% identity), *Physcomitrella patens*, which has extended sequences at both its N- and C-termini (Supplementary Fig. S1 at *JXB* online). Interestingly, phylogenetic analysis indicated that AAF was related more to monocots and *P. patens* than to dicots (Supplementary Fig. S2). However, AAF and its dicotyledon orthologues seem to have a chloroplast-targeted signal peptide as predicted by TargetP1.1 (http://www.cbs.dtu.dk/) (Supplementary Table S1).

To determine whether *AAF* is regulated by senescence factors, the expression pattern of *AAF* was analysed in four stages during leaf development. The expression of *AAF* was induced in early senescent leaves but not in mature green (MG) or late senescent leaves (Fig. 1A). *SAG12* was used as a senescence marker (Lohman *et al.*, 1994). Therefore, it was confirmed that *AAF* is also a SAG in *Arabidopsis*, similar to its orthologues in rice and sweet potato (Yap *et al.*, 2003). However, *AAF* was also expressed in young leaves (Fig. 1A, Y), which suggests that an additional function of *AAF* may be present in developmental stages other than organ senescence. To understand further the physiological role of *AAF* in non-senescent tissues, expression of *AAF* was analysed in different tissues. *AAF* was found to be expressed in flower buds, cauline leaves, rosette leaves, roots, and seedlings, but not in flowers, siliques, or stems, by RT-PCR analysis (Fig. 1B). Furthermore, histochemical staining of transgenic plants containing an *AAF* promoter fusion with the *uidA* gene encoding the enzyme GUS, *AAFpro::GUS*, was used to examine the expression of *AAF in planta*. *AAF* was expressed in the emerging true leaves (Fig. 1C, i and ii) and the elongation zone of primary and lateral roots in 7-day-old seedlings (i and iii). Moreover, *AAF* was expressed in cauline leaves (iv), young leaves (v), and senescent leaves (vii), but not in cotyledons (i), MG leaves (vi), or siliques (ix), which was fairly consistent with the expression profiles in Fig. 1B. Interestingly, *AAF* was expressed in the immature anthers of flower buds (Fig. 1C, viii; Fig. 1B, FB), but not in open flowers (Fig. 1B, F). Histochemical results indicated that *AAF* is expressed in various organs and leaves during different development stages and is not restricted to senescent leaves.

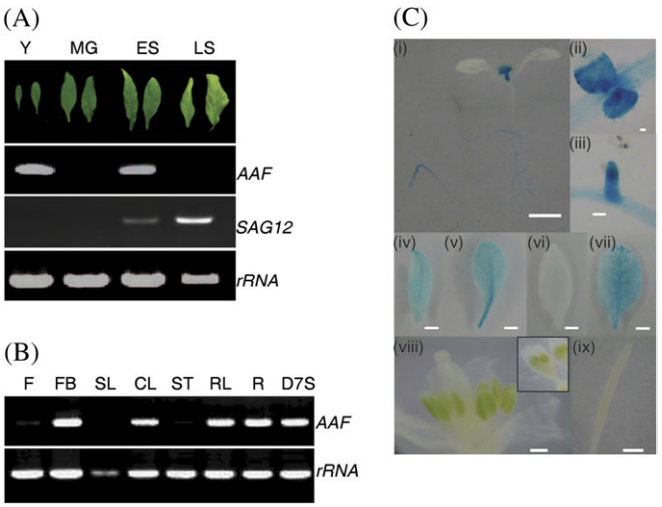

Fig. 1. Expression patterns of *AAF* in different developmental stages. (A) RT-PCR analysis of the *AAF* transcript in different stages of leaf development. Y, young; MG, mature green; ES, early senescence; LS, late senescence. (B) RT-PCR analysis of *AAF* in different organs. F, flowers; FB, flower buds; SL, siliques; CL, cauline leaves; ST, stems; RL, rosette leaves; R, roots; D7S, 7-day-old seedlings. Rosette leaves were taken from the aerial part of 5-week-old plants including Y and MG leaves. *18S rRNA* was used as a loading control in A and B. (C) GUS staining of transgenic *Arabidopsis* with the *AAFpro::GUS* construct. (i) Seven-day-old seedlings. (ii) First true leaves. (iii) Lateral roots. (iv) Cauline leaves. (v) Young leaves. (vi) Mature green leaves. (vii) Early senescent leaves. (viii) Immature flower buds. (ix) Siliques. Bars = 1 mm (i, iv, v, vi, vii, and ix) or 0.1 mm (ii, iii, and viii).

AAF is a plastid protein and the N-terminal signal peptide sequence is required for plastid targeting

Computational analysis with TargetP1.1 and ChloroP1.1 to predict the potential subcellular localization of AAF and its orthologues showed that all except for those in maize, rice, and moss have an N-terminal putative transit peptide for chloroplast localization (Supplementary Table S1 at *JXB* online) (Nielsen *et al.*, 1997; Emanuelsson *et al.*, 2000). AAF contains a 36-residue peptide at the N-terminus predicted as a chloroplast localization signal. To validate the prediction of AAF subcellular localization, AAF was fused with GFP under the control of the 35S promoter from CaMV, *CaMV35S::AAF:GFP*, and transient expression assays were performed with *Arabidopsis* mesophyll protoplasts. AAF:GFP was localized in chloroplasts (Fig. 2, top panel). Deletion of 40 residues at the N-terminus ($AAF_{41–417}$:GFP) to remove

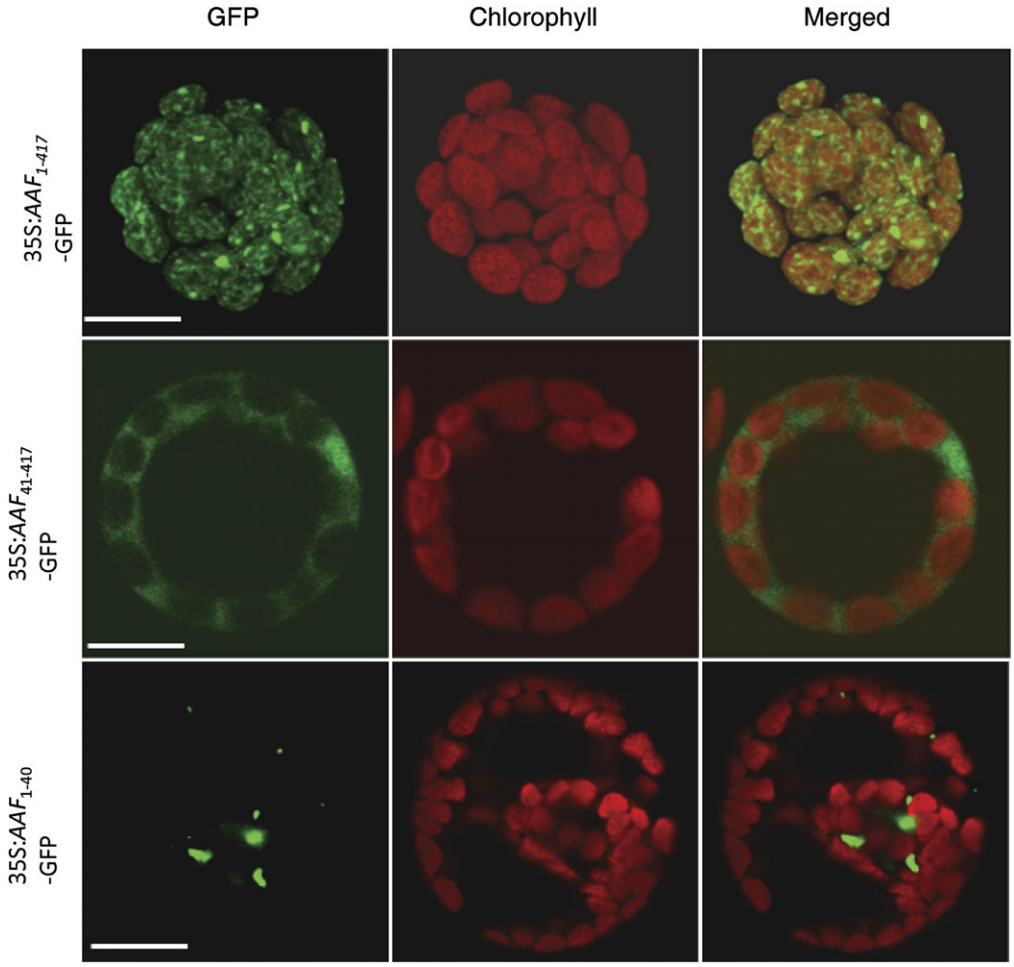

Fig. 2. Localization of *AAF* in chloroplasts. *Arabidopsis* mesophyll protoplasts were transfected with the following constructs: *35S::AAF*$_{1–417}$*–GFP* (top); *35S::AAF*$_{41–417}$*–GFP* (middle); and *35S::AAF*$_{1–40}$*–GFP* (bottom). First column: fluorescence images with pseudocolouir for GFP (green channel). Second column: autofluorescence of chloroplasts (red channel). Third column: merged micrographs of red and green images. Experiments were repeated three times and representative data are shown. Bars=10 μm.

the predicted transit peptide resulted in loss of chloroplast localization (Fig. 2, middle panel). However, the N-terminal 40 amino acids were not sufficient to direct the AAF$_{1–40}$:GFP fusion protein to chloroplasts (Fig. 2, bottom panel). Thus, AAF is a chloroplast protein in *Arabidopsis*, and the predicted transit peptide is essential but not sufficient for targeting to chloroplasts.

A 68-residue signal peptide for chloroplast targeting was predicted in SPA15 (Supplementary Table S1 at *JXB* online), suggesting the subcellular localization of SPA15 in plant cells. However, SPA15 was detected to associate specifically with the cell wall of various cell types, predominantly in senescent sweet potato leaves, by immunoelectron microscopic analysis (Yap *et al.*, 2003). To test the functionality of the predicted transit peptide in SPA15, a GFP fusion of *SPA15* under the control of the CaMV 35S promoter, *CaMV35S::SPA15:GFP*, was generated for a transient expression assay in *Arabidopsis* mesophyll protoplasts. The result indicated that the SPA15:GFP fusion protein was targeted to chloroplasts (Supplementary Fig. S3). Therefore, it is concluded that the predicted transit peptides in both AAF and SPA15 are functional chloroplast targeting signals.

Overexpression of AAF promotes leaf senescence, early flowering, and elongation of roots and root hairs

To investigate the functional role of *AAF* in *Arabidopsis*, multiple transgenic lines containing *CaMV35S::AAF* were generated and are referred to hereafter as *AAF* overexpression (*AAF-OX*) plants. Two independent transgenic lines, *AAF-OX1* and *AAF-OX2*, were selected that both showed a comparable level of ectopic expression of *AAF* (Fig. 3C). In addition, two independent T-DNA insertional mutants to homozygosity were identified and they were named *aaf-KO1* and *aaf-KO2* (Fig. 3A, B); both are null mutants by RT-PCR analysis (Fig. 3C).

Age-dependent senescence was analysed by using the third and fourth rosette leaves of individual plants in three assays, namely chlorophyll content, photochemical activity of PSII, and membrane ion leakage, from DAG28 (days after germination) to DAG49. The results revealed that age-dependent leaf senescence was promoted in *AAF-OX* but delayed in *aaf-KO* plants (Fig. 3D, E). Leaf yellowing and photosynthetic efficiency were first analysed by quantitative measurement of chlorophyll content and photochemical

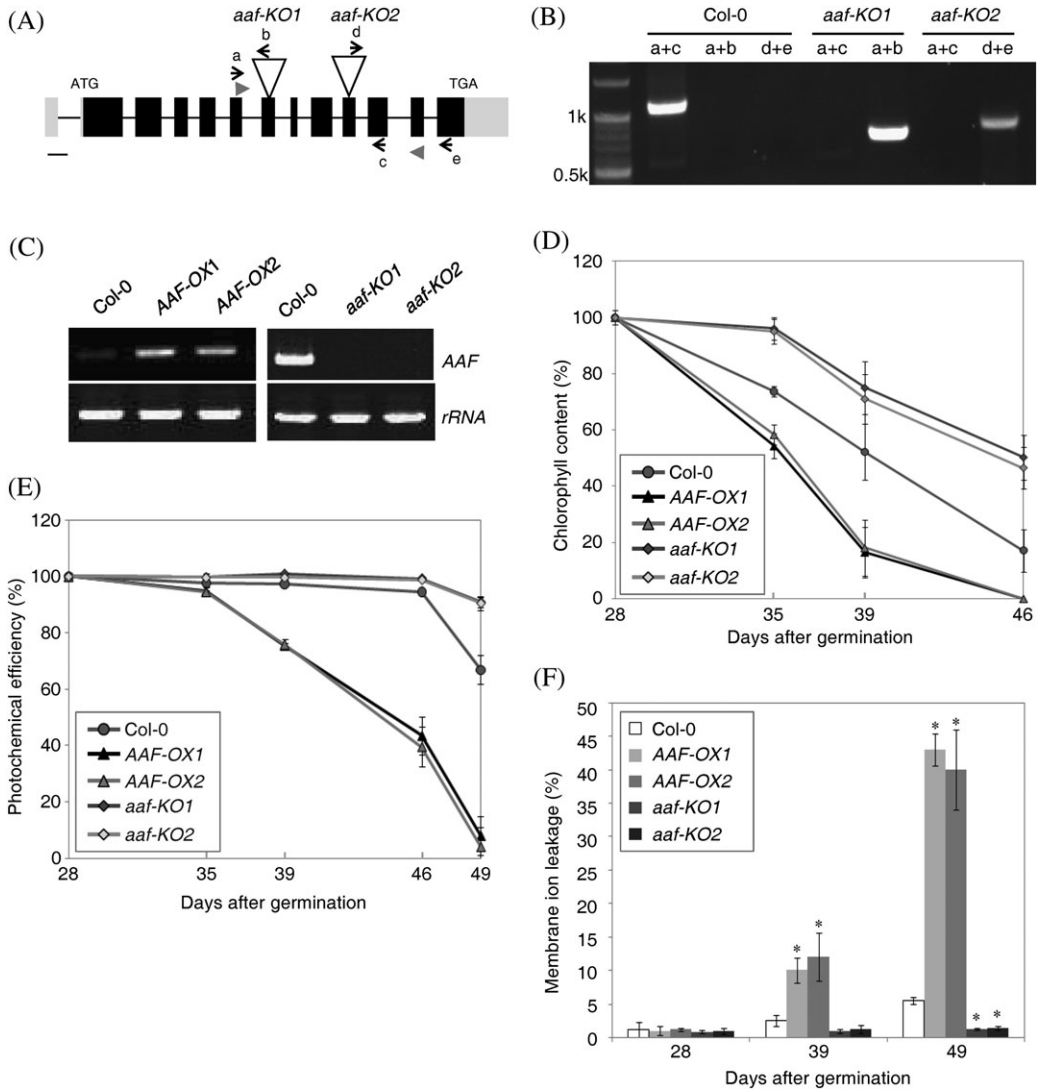

Fig. 3. Age-dependent senescence is promoted by overexpression of *AAF* but delayed in *aaf-KO* mutants. (A) The genomic structure of *AAF* and the T-DNA insertion sites for the *aaf-KO1* and *aaf-KO2* mutants. Filled boxes, exons; full lines, introns; grey boxes at both ends, the 5′- and 3′-untranslated regions. Bar=100 bp. (B) Genotyping of *aaf-KO1* and *aaf-KO2* with the primers a, b, c, d, and e indicated in A. (C) RT-PCR analysis to verify the presence of *AAF* transcript in *AAF-OX* (mature green leaves) and *aaf-KO* (flower buds). *AAF* transcript was amplified by a pair of gene-specific primers, AAF-F and AAF-R, represented by arrowheads in A. The third and fourth leaves were collected from plants at the number of days after germination as indicated to analyse age-dependent leaf senescence by measuring the levels of chlorophyll content (D), photochemical efficiency of PSII (E), and membrane ion leakage (F). *P <0.01 versus the wild type, Col-0 (n=4–6). The measurement of chlorophyll content (D) and photochemical activity (E) was set as 100% at 28 days after germination for comparison with samples collected thereafter.

activity, respectively. The chlorophyll content of rosette leaves was reduced to 54–58% in *AAF-OX*, 74% in the wild type (Col-0), and 95–96% in *aaf-KO* at DAG35 when compared with those in 4-week-old plants (100% at DAG28) (Fig. 3D). It was observed that the chlorophyll content was gradually reduced to a complete loss in *AAF-OX1* and *AAF-OX2* at DAG46, while 17% and 46–50% of chlorophyll levels remained in wild-type and *aaf-KO* plants, respectively (Fig. 3D). In addition, the photochemical activity of PSII began to show a reduction in *AAF-OX* at DAG39 and reached barely detectable levels at DAG49, while it was retained at 67% and 90% in the wild type and *aaf-KO*, respectively, at DAG49 (Fig. 3E). Next the electrolyte leakage was measured to analyse the membrane integrity of cells in senescent leaves. It was found that *AAF-OX* transgenics showed a significant increase in membrane ion leakage by 10–12% and 40–43% at DAG39 and DAG49, respectively, when compared with a mere 5% increase in the wild type at DAG49 (Fig. 3F). The levels of electrolyte leakage in *aaf-KO* were barely detectable at the same growth stages. Moreover, the expression of *SAG12* and *SAG13* was up-regulated in *AAF-OX* and not expressed in *aaf-KO* when compared with 7-week-old wild-type plants by RT-PCR analysis (Supplementary Fig. S4C at *JXB* online). By using

three different assays to evaluate the role of AAF involved in age-dependent leaf senescence, it was revealed that overexpression of *AAF* promoted, and deletion of *AAF* delayed, leaf senescence, and *AAF* was required for the expression of *SAG12 and SAG13* in 7-week-old plants.

In addition to promoting early senescence in leaves, *AAF-OX* showed an early flowering phenotype (Fig. 4A). The flowering time of *AAF-OX* was approximately at 22 d and 39 d as compared with 28 d and 48 d for the wild-type under LD and SD conditions, respectively (Fig. 4B). The wild type and *aaf-KO* did not significantly differ in flowering time. In addition, the roots of 5-day-old *AAF-OX* seedlings were ~40% longer than those in the wild type and *aaf-KO* (Fig. 4C, D). *AAF-OX* seedlings also showed an enhanced development of root hairs by ~40% more than in the wild type (Fig. 4E, F). However, wild-type and *aaf-KO* seedlings did not differ in root length and root hair development.

Accelerated leaf yellowing and degradation of chloroplasts in AAF-OX by continuous darkness

Next, it was decided to determine whether *AAF* is also involved in leaf senescence induced by stress. Continuous darkness acts as an inducer of leaf senescence in whole plants and detached leaves (Weaver and Amasino, 2001; Lin and Wu, 2004). *AAF-OX* showed enhanced leaf yellowing after continuous darkness for 5 d, whereas *aaf-KO* showed delayed leaf yellowing as compared with the wild type in whole plants (data not shown). To quantify the leaf senescence induced by continuous darkness, the fifth and sixth leaves detached from 4-week-old plants were used for the three senescence assays described above. The chlorophyll content of *AAF-OX1* and *AAF-OX2* was reduced dramatically to 4% and 5% of that at day 0 (100% at day 0), respectively, after a 5 d dark treatment, as compared with 31% in the wild type, whereas that in *aaf-KO1* and *aaf-KO2*

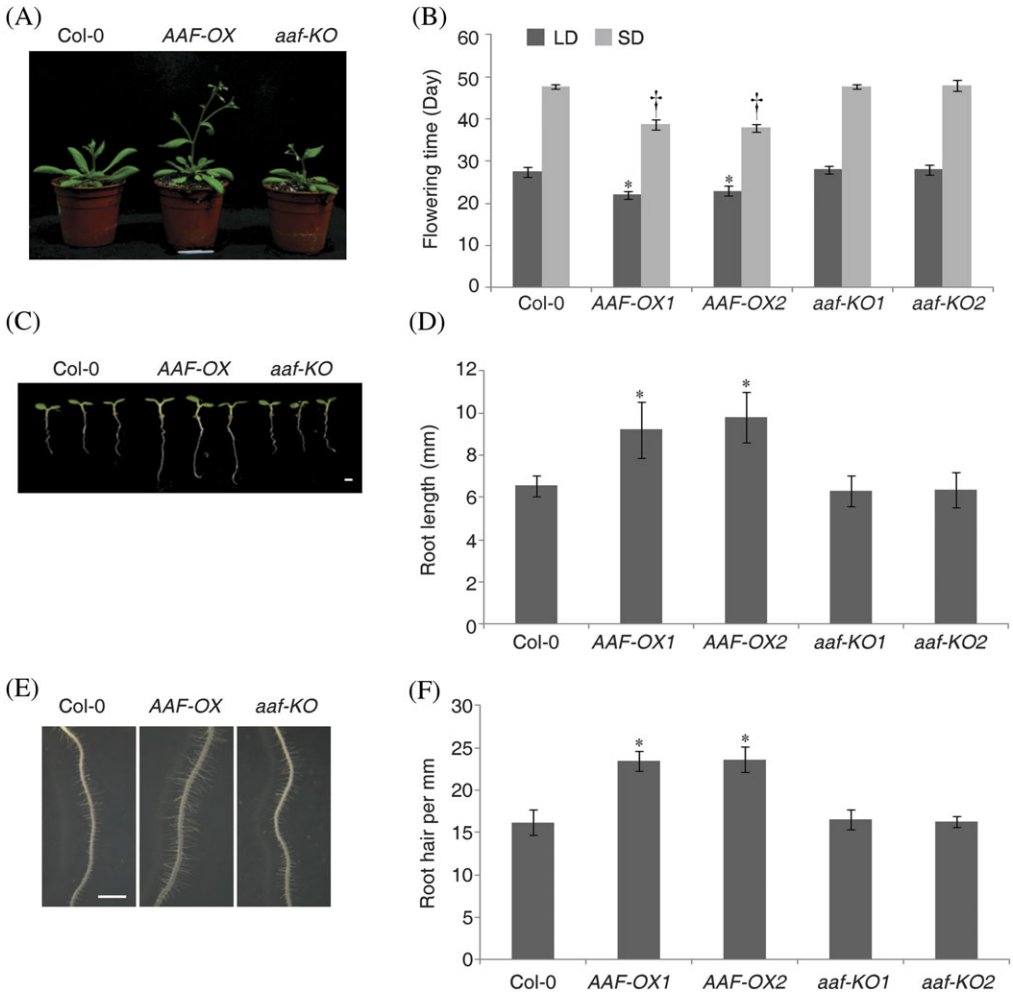

Fig. 4. Overexpression of *AAF* promotes early flowering and root growth. (A) Analysis of the flowering phenotype of 33-day-old plants cultivated under long-day conditions. (B) Flowering time under long-day (LD, black) or short-day (SD, grey) conditions. **P* <0.01 (LD) and †*P* <0.01 (SD) versus the wild type, Col-0. Data represent means ±SE (*n*=6). (C) Root phenotype of 5-day-old seedlings grown under white light in long-day conditions. (D) Length of primary roots of 5-day-old seedlings. (E) Images of root hairs in a region 1.5 mm from the root tip in D. (F) Root hair density of 5-day-old seedlings. Data represent means ±SE (*n*=23–29) in D and F. **P* <0.01 versus the wild type, Col-0. Bars=1 mm.

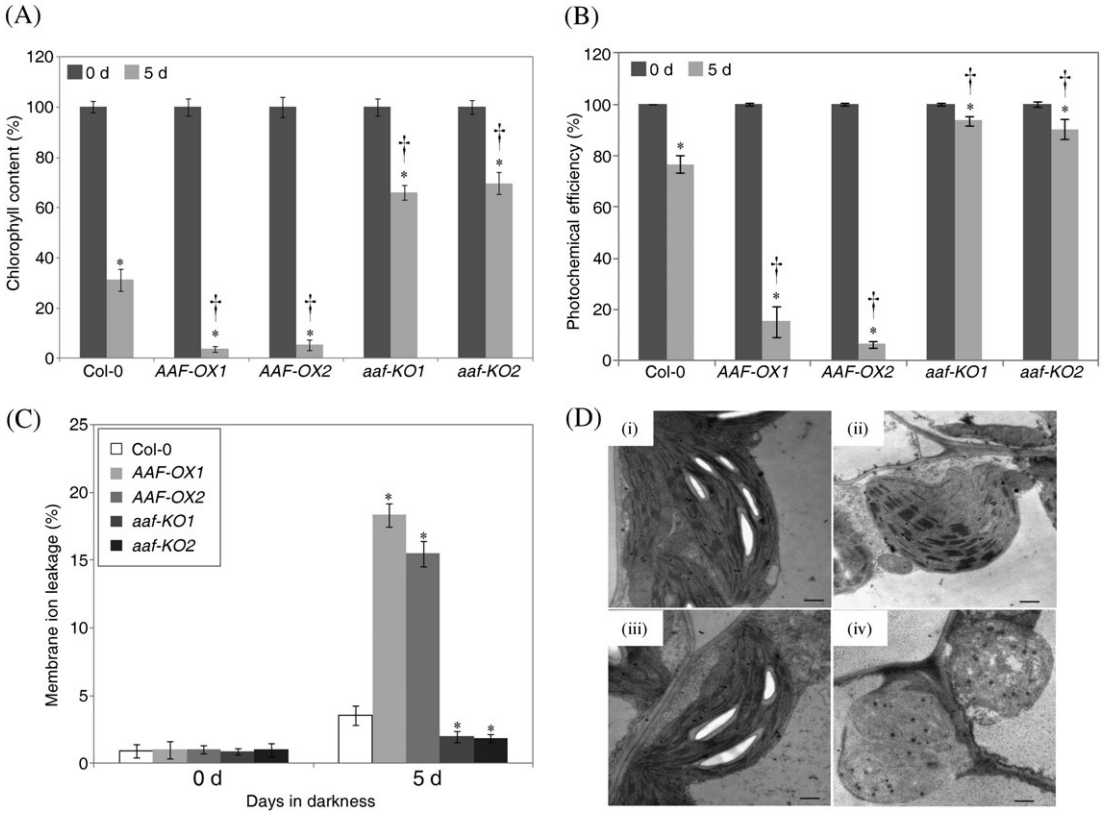

Fig. 5. Leaf senescence induced by continuous darkness is enhanced in *AAF-OX*. (A–C) Dark-induced senescence was analysed by using detached leaves from 4-week-old plants. The fifth and sixth leaves were excised and incubated in darkness for 5 d followed by measuring the chlorophyll content (A), photochemical efficiency (B), and membrane ion leakage (C). **P* <0.01, 5 d versus 0 d (*n*=6); †*P* <0.01, *AAF-OX* or *aaf-KO* versus the wild type (Col-0) by the percentage of chlorophyll reduction after dark treatment (*n*=6). Data represent means ±SE. (D) Electroscopic analysis of 3-week-old plants treated with continuous darkness for 5 d (ii and iv; wild type and *AAF-OX*, respectively) or without dark treatment (i and iii; wild type and *AAF-OX*). Bars=0.5 μm.

was reduced to 66% and 69%, respectively (Fig. 5A). Analyses of the photosynthetic efficiency indicated that overexpression of *AAF* resulted in reduction in photochemical activity to 85–90% after a 5 d dark treatment, whereas only an ~23% and a <10% reduction was observed in wild-type and *aaf-KO* plants, respectively (Fig. 5B). In addition, the electrolyte leakage was increased to 18% and 15% in *AAF-OX1* and *AAF-OX2*, respectively, and <4% in the wild type and 2% in *aaf-KO* plants after dark treatment (Fig. 5C). Thus, overexpression of *AAF* promoted, but loss of *AAF* function in *aaf-KO* delayed, leaf senescence induced by continuous darkness.

Transmission electron microscopy was then used to examine whether the ultrastructure of chloroplasts is affected by darkness. The wild type and *AAF-OX* did not differ in chloroplast ultrastructure before dark treatment; both showed intact grana and thylakoids, comparable size and/or number of starch grains, and a few plastoglobuli (Fig. 5D, i and iii). After a 5 d dark treatment, wild-type chloroplasts became spherical and lacked starch grains, but the granal stacking remained (Fig. 5D, ii). However, the chloroplasts of *AAF-OX* showed complete loss of starch grains and grana, and a deformed shape with rupture of membranes, which led to hollow stroma in severe cases and increased accumulation of plastoglobuli (Fig. 5D, iv). Therefore, darkness-induced chloroplast degradation was enhanced in *AAF-OX*.

Global gene expression analysis reveals that AAF is involved in redox homeostasis

To understand the function of *AAF* at the gene expression level, transcriptome profiles were analysed in leaves of 3-week-old *AAF-OX* by microarray experiments. Genes with differential expression in the wild-type and *AAF-OX* plants with a cut-off at 1.5-fold were selected for GO analysis. Fisher's test was used to calculate the significance of the percentage distribution of GO annotations for comparison with those in the whole genome. Genes regulated by *AAF-OX* in the distribution of GO annotation are highly related to 'response to stress' and 'response to abiotic or biotic stimulus', with a *P*-value of 1.96×10^{-17} and 1.52×10^{-12}, respectively (Fig. 6A), which suggests that genes responsive to stress are overrepresented in *AAF-OX*. Moreover, genes regulated by *AAF-OX* were highly related to 'oxidation reduction' and 'oxidative stress', with a *P*-value of 5.34×10^{-19} and 4.69×10^{-5}, respectively (Fig. 6B). Results from transcriptome analysis suggested that *AAF* is involved in regulation of redox status responding to various stress

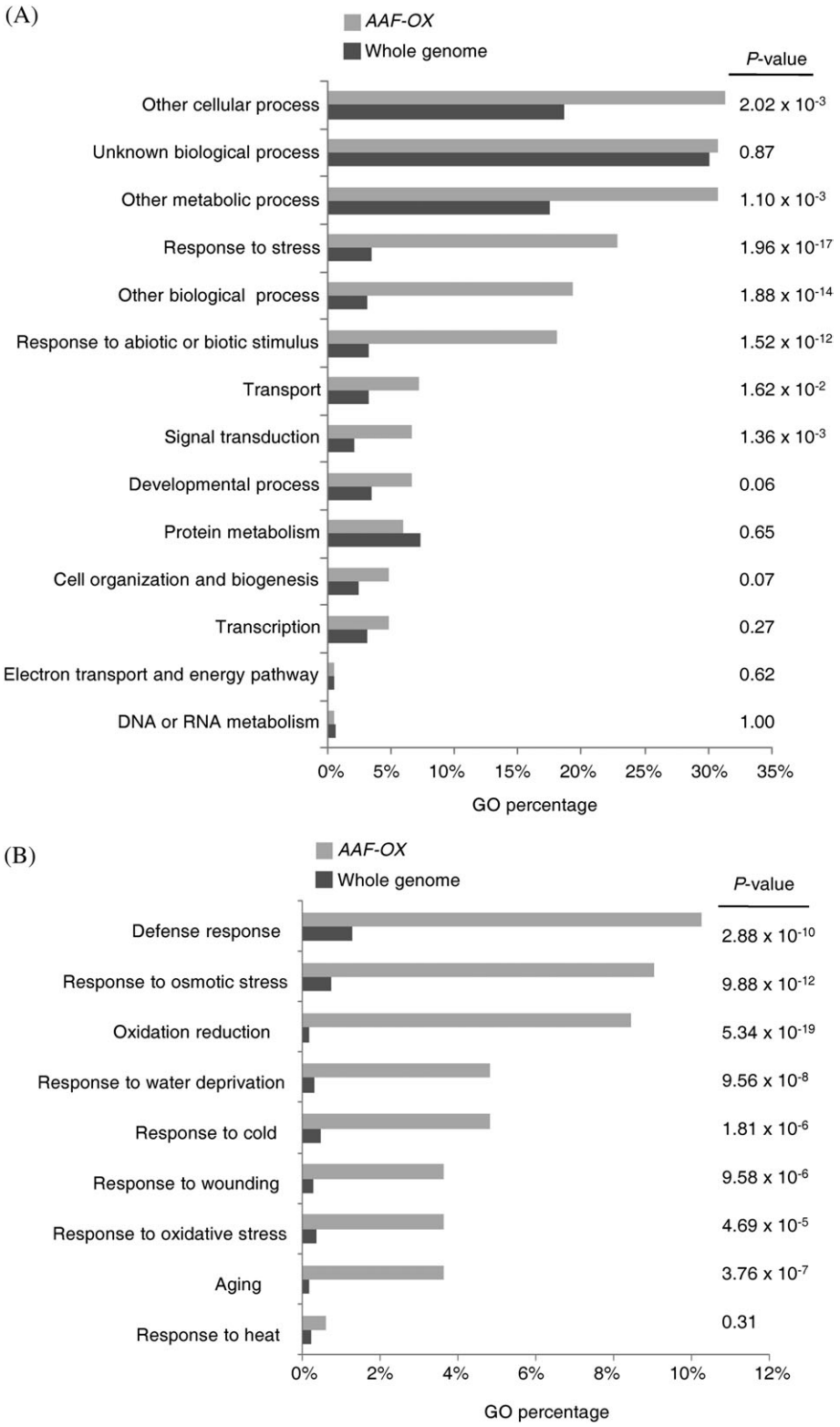

Fig. 6. Global analysis of gene expression profiles in *AAF-OX*. (A) Expression profiles of genes up-regulated in *AAF-OX* by analysis based on the Gene Ontology (GO) annotation (biological process) in TAIR. (B) Analysis of genes induced in *AAF-OX* by specific GO terms. *P*-values in A and B were calculated by Fisher's test to compare the percentage distribution of GO annotation from genes induced by *AAF-OX* and the whole genome.

conditions in *Arabidopsis*. Further analysis indicated that several groups of genes involved in 'defence response', 'response to osmotic stress', 'response to water deprivation', 'response to cold', 'response to wounding', and 'ageing' were significantly overrepresented in *AAF-OX* as compared with the whole genome (Fig. 6B). However, *AAF* may not be

involved in all types of stress response, such as heat stress (Fig. 6B).

To verify whether the differentially expressed genes identified from microarray data were up-regulated in *AAF-OX*, the expression levels of selected genes were examined by real-time PCR analysis (Table 1). Defence genes such as *LTP4*, *PDF1.2b*, and *PDF1.2a* were ~19.73-, 73.9-, and 48.22-fold more highly expressed, respectively, in *AAF-OX* than in the wild type (Table 1). *AtERF1* and *HEL*, classified as defence genes and also regulated by ethylene, were induced by 8.87- and 4.19-fold, respectively, in *AAF-OX*. In addition, the expression of several senescence-associated genes, such as *SAG12*, *SAG13*, *CHITINASE*, and *SEN1*, and oxidative stress-related genes, such as those encoding glutathione *S*-transferase and peroxidase, were up-regulated in *AAF-OX* (Table 1). Thus, overexpression of *AAF* may interfere with cellular redox homeostasis to induce stress- and senescence-related genes at the developmental stage before senescence.

Overexpression of AAF in Arabidopsis *leads to accumulation of ROS*

Because of the similar phenotypes and expression levels (Figs 3–5) of ectopically expressed *AAF* in two independent transgenic lines, *AAF-OX1* was used as a representative transgenic for further characterization in subsequent experiments. Similarly, one of the two null mutants of *AAF*, *aaf-KO2*, was selected for phenotypic analyses hereafter. Since oxidative stress-related genes were significantly overrepresented in those up-regulated in *AAF-OX*, it was reasoned that overexpression of *AAF* may result in changes in cellular redox poise and/or altered response to ROS levels. First, the H_2O_2 level was analysed in young and MG leaves by using DAB for histochemical staining. It was previously shown that *AAF* is expressed in young but not MG leaves in the wild type (Fig. 1A) and the slightly expressed *AAF* does not lead to accumulation of sufficient H_2O_2 to be detected by DAB staining (Fig. 7A). However, the young and MG leaves in *AAF-OX* showed a dense DAB staining, which indicates that an elevated level of H_2O_2 was induced by overexpression of *AAF* (Fig. 7A). *aaf-KO* plants revealed neither gene expression of *AAF* nor DAB staining of H_2O_2. With real-time PCR analysis used to quantify the expression levels of *AAF*, a 25.2- and 23.2-fold increase in *AAF* expression was found in young and MG leaves of *AAF-OX*, respectively, as compared with MG leaves of the wild type (Fig. 7B). Thus, the 3.15-fold elevated *AAF* expression in young leaves of the wild type was not sufficient to induce H_2O_2 accumulation, as visualized by DAB staining. Quantification of the H_2O_2 level indicated ~29% more H_2O_2 in *AAF-OX* plants than in the wild-type and *aaf-KO* plants (Fig. 7C). A fluorescence probe, DCFDA, was next used to detect ROS in roots of seedlings. The roots of *AAF-OX* showed more fluorescence than did those of the wild type or *aaf-KO*, which suggests a significant accumulation of ROS in the roots of *AAF-OX* (Fig. 7D). Because only non-pigmented plastids (leucoplasts) are present in roots, elevated levels of ROS by overexpression of *AAF* can be induced independently of photosynthesis. Lipid peroxidation resulting from oxidative degradation of polyunsaturated fatty acids in lipids by ROS was next analysed by measuring the levels of MDA, an end-product of oxidized lipids. Approximately 30% more MDA was generated in the leaves of *AAF-OX* as compared with those of the wild type and *aaf-KO* (Fig. 7E). The use of four different assays to analyse ROS levels demonstrated that overexpression of *AAF* promoted ROS accumulation in rosette leaves and roots.

AAF is involved in response to oxidative stress

Overexpression of *AAF* promotes ROS accumulation and induces leaf senescence during development (Fig. 3D–F) and on exposure to darkness (Fig. 5). It was surmised that

Table 1. Defence-, senescence-, and oxidative stress-related genes are up-regulated in 3-week-old *AAF-OX*

Function	AGI number	Description	Fold change[a]	RER[b]
Defence	At5g59319	Lipid transfer protein (LTP4)	17.42	19.73±1.36
	At2g26020	Plant defensin (PDF1.2b)	14.7	73.9±11.10
	At5g44020	Plant defensin (PDF1.2a)	11.17	48.22±7.20
	At3g04720	Hevein-like protein (HEL)	3.03	8.87±1.27
	At4g17500	ATERF1	1.74	4.19±0.46
Senescence	At5g45890	Cysteine proteinase (SAG12)	32.31	65.01±4.77
	At2g43570	Chitinase, putative	5.99	17.82±1.87
	At2g29350	Alcohol dehydrogenase (SAG13)	2.06	29.16±9.61
	At3g45590	SEN1	1.67	2.04±0.33
Oxidative stress	At5g37940	NADP-dependent oxidoreductase, putative	4.28	2.59±0.30
	At1g02920	Glutathione *S*-transferase	2.14	12.3±0.39
	At1g06290	Acyl-CoA oxidase (ACX3)	1.85	1.85±0.99
	At4g37520	Peroxidase	1.62	9.8±2.40
	At5g58390	Peroxidase	1.56	3.41±0.51

[a] Fold change is the mean of two independent experiments with the ratio of raw signal values in *AAF-OX* and the wild type. The raw data are available in the GEO database with the accession no. GSE18336.

[b] Gene expression levels were quantified by real-time PCR and the relative expression rate (RER) was compared between *AAF-OX* and the wild type. Data represent means ±SE (n=3).

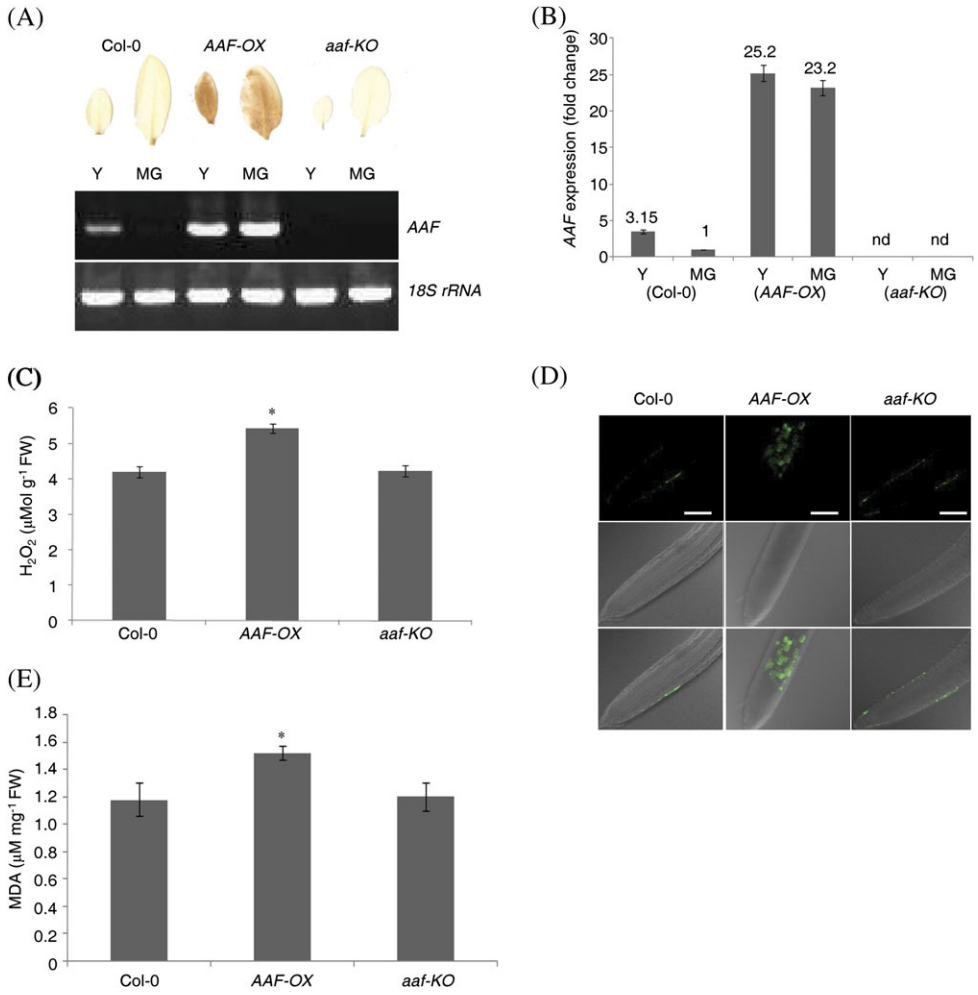

Fig. 7. ROS are accumulated in *AAF-OX*. (A) Histochemical staining by DAB of H_2O_2 in young (Y) and mature green leaves (MG) from 3-week-old plants. RT-PCR analysis of *AAF* expression levels from plants of the same developmental stages. (B) Real-time PCR analysis of *AAF* expression levels in 3-week-old plants. All transcripts were normalized to *ACTIN2* expression as a reference gene, and MG of the wild type (Col-0) was set as 1. Data represent means ±SE (n=6). nd, not detected, in *aaf-KO* plants. (C) Analysis of H_2O_2 levels in rosette leaves from 3-week-old plants using the Amplex Red kit. (D) Analysis of ROS levels in the roots of 7-day-old seedlings by DCFDA. Panels at the top, images of fluorescence in pseudocolour; middle, DIC images; bottom, merged images. Bars=50 μm. (E) Analysis of lipid peroxidation in 3-week-old plants by quantification of malondialdehyde levels. *P <0.01 versus the wild type, Col-0 in C and E; data represent means ±SE (n=6).

the elevated levels of ROS in *AAF-OX* might result in hypersensitivity to oxidative stress and therefore lead to leaf senescence. Thus, the chlorophyll content was measured in detached leaves as an indicator of senescence in the presence of reagents to induce oxidative stress. Detached leaves were floated in MES buffer supplemented with 10 mM H_2O_2 for 3 d before the chlorophyll content was measured. *AAF-OX* showed a significant loss of chlorophyll (42% of day 0) as compared with the wild type (64% of day 0) and *aaf-KO* (84% of day 0) (Fig. 8A), which indicated that *AAF-OX* was hypersensitive and *aaf-KO* was hyposensitive to exogenous H_2O_2. It was next asked whether the overexpression of *AAF* becomes more sensitive to ROS generated endogenously by treatment with paraquat (methyl viologen), which perturbs cyclic electron flow in PSI to generate superoxide, a major ROS, during photosynthesis. Detached leaves from *AAF-OX* showed severe chlorophyll loss in the presence of 12.5 μM paraquat for 2 d. Quantification of the chlorophyll content revealed a marked reduction, to 22% of that on day 0, in *AAF-OX* treated with paraquat as compared with 63% and 79% in the wild type and *aaf-KO*, respectively (Fig. 8B). These results suggest that *AAF* is involved in the response to cellular redox status. Therefore, ectopic expression of *AAF* in *AAF-OX* plants results in hypersensitivity and a null mutation in *aaf-KO* hyposensitivity to oxidative stress induced by H_2O_2 and paraquat. The hypersensitivity to ROS-inducing agents in *AAF-OX* may be due to an elevated endogenous H_2O_2 level and lipid peroxidation even in the absence of any oxidative stress (Fig. 7C, E).

A functional EIN2 is required for the enhanced senescence phenotype in AAF-OX

The role of ethylene in promoting leaf senescence in plant species is well known (Grbi'c and Bleecker, 1995). The

EIN2 gene encodes a master positive regulator in the ethylene signalling pathway and is involved in response to oxidative stress (Alonso *et al.*, 1999; Jing *et al.*, 2002; Cao *et al.*, 2006). Mutations in *EIN2* delayed leaf senescence (Grbi'c and Bleecker, 1995) and resulted in constitutive activation of several antioxidant enzymes that conferred enhanced resistance to oxidative stress (Alonso *et al.*, 1999; Cao *et al.*, 2006). Microarray analysis from this study also revealed that several ethylene-responsive genes, such as *PDF1.2a*, *AtERF1*, and *HEL1*, were up-regulated in *AAF-OX* (Table 1). To investigate whether *EIN2* is involved in the function of *AAF* in response to oxidative stress to accelerate leaf senescence, *ein2-5* was introduced into *AAF-OX* by a genetic cross to generate *AAF-OX/ein2-5*. Detached leaves from 3-week-old plants were floated in MES buffer and treated with continuous darkness for 5 d to analyse chlorophyll levels. *AAF-OX* was more sensitive to dark treatment, with the chlorophyll content reduced to 24% of that on day 0, but the content was 49% and 73% in the wild type and *ein2-5*, respectively (Fig. 8C). However, the level of chlorophyll was reduced to only 64% in *AAF-OX/ein2-5*, which indicates that *ein2-5* recovered the chlorophyll loss in *AAF-OX* induced by darkness (Fig. 8C). In the presence of 20 mM H_2O_2, the chlorophyll content was reduced to 29% of that on day 0 in *AAF-OX* and 57% in the wild type (Fig. 8D). Surprisingly, neither *ein2-5* nor *AAF-OX/ein2-5* was affected by exogenous H_2O_2 (Fig. 8D). Finally, flotation of detached leaves on 50 μM paraquat for

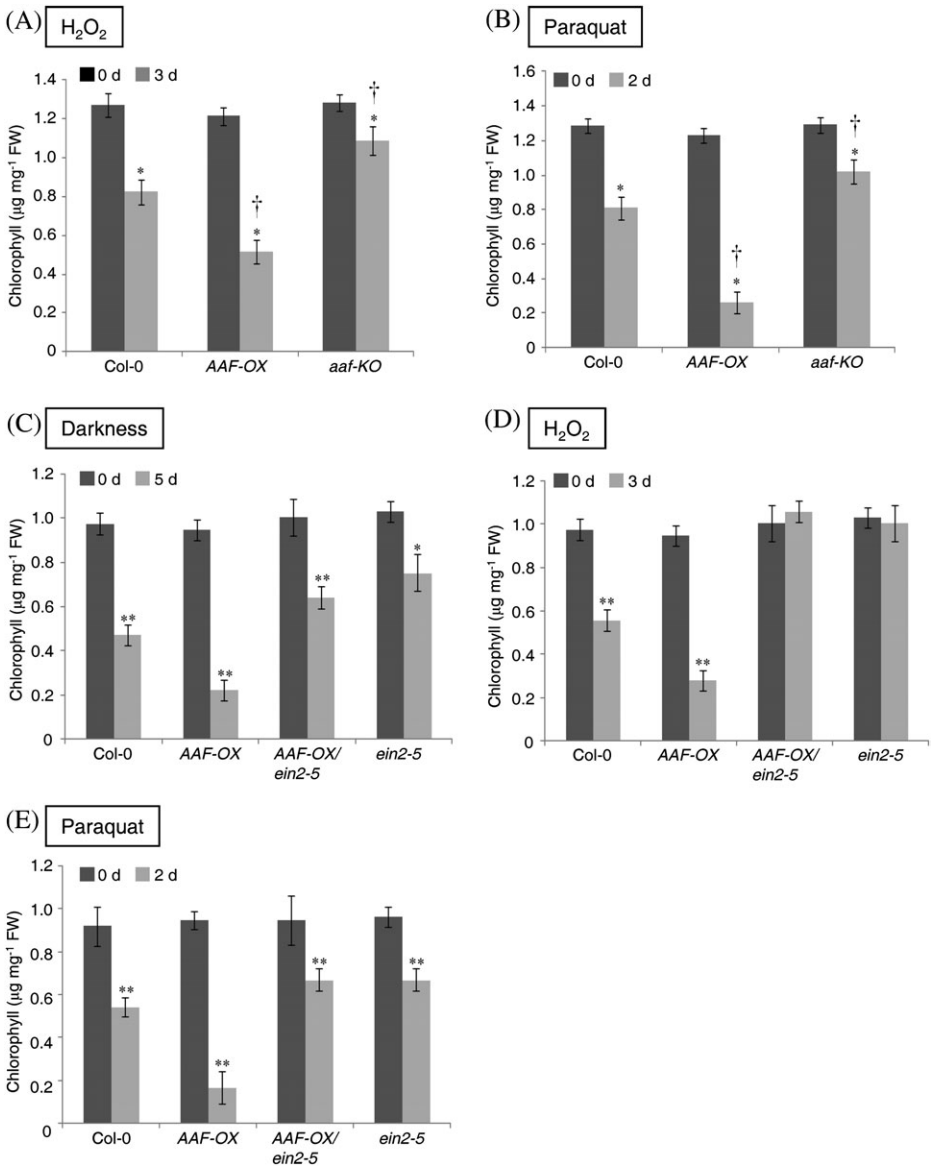

Fig. 8. Enhanced sensitivity to oxidative stress in *AAF-OX* is dependent on a functional *EIN2*. Chlorophyll content of detached leaves was quantitated in the absence and presence of (A) 10 mM H_2O_2 for 3 d; and (B) 12.5 μM paraquat for 2 d. **P* <0.01 versus 0 d; †*P* <0.01, *AAF-OX* or *aaf-KO* versus the wild type, Col-0. Data represent means ±SE (*n*=6). Chlorophyll content of detached leaves treated with (C) continuous darkness for 5 d; (D) 20 mM H_2O_2 for 3 d; (E) 50 μM paraquat for 2 d. **P* <0.05 or ***P* <0.01 versus the wild type, Col-0. Data represent means ±SE (*n*=6).

2 d resulted in significant chlorophyll loss in *AAF-OX*, with a reduction to 17% of that on day 0 and 59% in the wild type (Fig. 8E). Both *ein2-5* and *AAF-OX*/*ein2-5* showed a similar reduction in chlorophyll content, to 70% (Fig. 8E). Thus, *ein2-5* apparently suppresses the chlorophyll loss in *AAF-OX* induced by darkness and oxidative stress. Therefore, a functional *EIN2* is required for *AAF* to respond to oxidative stress and continuous darkness to promote the subsequent senescence in leaves.

Expression of AAF is induced by ACC in Arabidopsis seedlings

Several stress hormones have been studied for their roles in age-dependent and/or stress-induced leaf senescence by an extensive and comparative microarray analysis (Buchanan-Wollaston *et al.*, 2005). Among the stress-related hormones, ethylene, JAs, SA, and ABA have been shown to promote leaf senescence responding to developmental, pathogen-, or dark-induced signals (Grbi'c and Bleecker, 1995; Morris *et al.*, 2000; He *et al.*, 2002; Cho *et al.*, 2009). Overexpression of *AAF* in *Arabidopsis* is sensitive to oxidative stress that requires a functional *EIN2* (Fig. 8C–E). Yap *et al.* (2003) showed that expression of *SPA15* was significantly induced by ethylene in detached sweet potato leaves. It is possible that the expression of *AAF* is induced by ethylene in *Arabidopsis*. To test this possibility, 7-day-old light-grown seedlings treated with ACC (100 μM) were used and samples were collected at the designated time points for preparation of total RNA. Expression of *AAF* was induced 2-fold by ACC at 1 d after treatment, and the induced level continued for 3 d in the presence of ACC. *AAF* expression was not induced in *ein2-5*, suggesting that a functional ethylene response is required for the induction of the *AAF* gene by ACC (Fig. 9A). *ERF1*, an early ethylene-responsive gene, was used as a control, and its expression was induced ~4-fold at 6 h by ACC in the wild type, but not in *ein2-5* (Fig. 9B). These data support that expression of *AAF* can be induced by ethylene and suggest a potential positive feedback regulation of AAF function by the ethylene signalling pathway.

Discussion

Leaf senescence is regulated by different factors resulting from developmental and environmental signals. Here a study of the physiological roles of *AAF* in age-dependent, dark-induced, and oxidative stress-promoted leaf senescence in *Arabidopsis* is reported. The data support that overexpression of *AAF* promotes leaf senescence involving response to ROS that is dependent on a functional *EIN2*, and a null mutation in *aaf-KO* delays leaf senescence and becomes more resistant to oxidative stress. The expression of *AAF* is regulated by age-dependent senescence factors and is probably involved in stress response and pathogen defence based on transcriptome analysis. The interplay of the endogenous and exogenous factors may regulate the expression of *AAF* to modulate ROS homeostasis and/or modify sensitivity to oxidative stress, thus leading to leaf senescence dependent on *EIN2*. Furthermore, because the expression of *AAF* is not limited to senescent leaves, *AAF* may also be involved in regulating plant growth and development prior to organ senescence by modulating redox homeostasis. The current work demonstrates that a functional *EIN2* or ethylene pathway is required for *AAF* to respond to darkness and oxidative stresses to induce leaf senescence. Whether additional signals from environmental stresses or phytohormones are relayed to *AAF* to regulate cellular redox homeostasis remains to be investigated.

The gradual loss of antioxidant capacity is one of the pivotal factors resulting in ageing in animals and plants. ROS production and accumulation has been shown to be associated with leaf senescence in plants (Procházková and Wilhelmová, 2007). Results from the current work suggest that there are two possible roles of AAF that may be linked to ROS to regulate leaf senescence; one is that AAF directly modulates ROS levels to regulate cellular redox homeostasis (Fig. 7) and the other is the differential sensitivities to oxidative stress or elevated ROS levels conferred by different expression levels of *AAF* (Fig. 8). Analysis of the ROS levels in *aaf-KO* and the wild type at the senescent stage will provide important information to delineate the role of AAF during leaf senescence. Previous reports indicated that mutants with increased tolerance to oxidative stress had

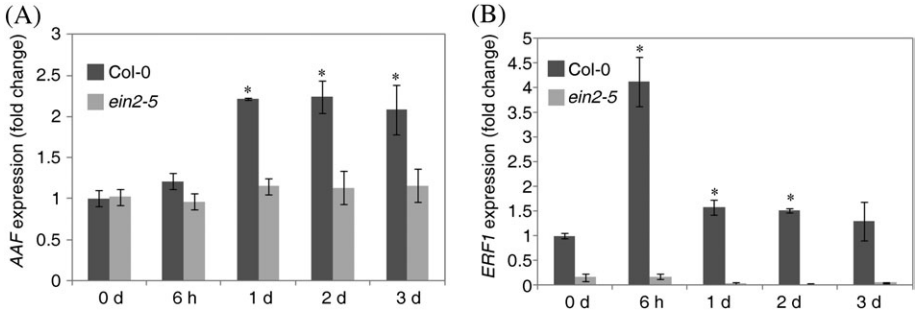

Fig. 9. Expression of *AAF* is induced by ACC. Expression levels of *AAF* (A) and *ERF1* (B) were quantified by real-time PCR in 7-day-old light-grown seedlings of Col-0 and *ein2-5* in the absence and presence of 100 μM ACC. Samples of total RNA were prepared from seedlings collected at the indicated times. Data were normalized to the expression of *ACTIN2* (At3g46520). Fold change of Col-0 at 0 day was set as 1. *P <0.01 versus the wild type, Col-0 at 0 d. Data represent means ±SE (n=3).

extended leaf longevity or showed a late flowering phenotype (Kurepa *et al.*, 1998; Woo *et al.*, 2004). While it did not show the late flowering phenotype (Fig. 4A), *aaf-KO* exhibited increased tolerance to oxidative stress and delayed leaf senescence (Figs 3D–F, 5A–C, 8A, B). The *Arabidopsis ore1*, *ore3*, and *ore9* mutants characterized by Woo *et al.* (2004) showed increased leaf longevity and enhanced tolerance to several ROS-inducing agents. The regulatory mechanism in the *ore* mutants was suggested to be the altered response to oxidative stress instead of modulated activity of antioxidant enzymes. The nature of AAF function in leaf senescence involving redox homeostasis requires further research and it may also have a similar role to the *ore* mutants in plant physiology. Interestingly, *ore3* is a mutation allele in *EIN2*, which is required for the action of AAF in modulation of leaf senescence (Fig. 8C–E). On the other hand, studies on *xdh1* (Brychkova *et al.*, 2008) and *cpr5/old1* (Jing *et al.*, 2008) revealed that elevated cellular ROS levels resulted in accelerated leaf senescence.

The present results (Figs 3, 5) indicated that *AAF-OX* and *aaf-KO* promoted and delayed leaf senescence, respectively, in both age-dependent (4- to 7-week-old plants, Fig. 3) and darkness-induced (3-week-old plants, Fig. 5) conditions. On the basis of GO analysis from microarray data (Fig. 6), it was hypothesized that AAF was also involved in response to or modulation of ROS levels in stress-induced senescence in leaves. It was found that *AAF-OX*, but not *aaf-KO* plants, showed visible phenotypes in flowering time (Fig. 4A, B, 5-week-old plants), elongation of primary roots, and development of root hairs (Fig. 4C–F, 5-day-old seedlings). When the ROS levels were measured, only *AAF-OX* showed elevated levels of H_2O_2 and MDA in the rosette leaves of 3-week-old plants (Fig. 7C, E) and in the roots of 7-day-old seedlings (Fig. 7D). Results from phenotypic analyses (Fig. 4) and measurements of ROS levels (Fig. 7) were obtained by using transgenic plants prior to their showing developmental senescence in leaves. It was argued that ROS levels were tightly regulated and maintained homeostasis in the young and/or unstressed plants and ROS homeostasis would be disrupted by loss of antioxidant capacity or increased ROS production in senescent and stressed plants. Therefore, *AAF-OX* can promote ROS accumulation and/or increase response to ROS levels in both young and senescent plants. However, *aaf-KO* will not show visible phenotypes unless plants are stressed (Fig. 8A, B) or enter the senescent stage at a later time (Fig. 3D–F), which may be because *aaf-KO* is more tolerant to oxidative stress than wild type.

Flowering time and development of root hairs influenced in AAF-OX

Ascorbic acid (AsA) is an important antioxidant that detoxifies H_2O_2 to water. AsA-deficient mutants (*vtc1*, *vtc2*, *vtc3*, and *vtc4*) have shown that the levels of AsA in *Arabidopsis* modulate the expression of genes in the flowering pathways to promote early flowering and enhance premature leaf senescence (Kotchoni *et al.*, 2009). An early flowering phenotype was shown in *AAF-OX* (Fig. 4A, B), which may be due to elevated ROS levels and decreased levels of antioxidants such as AsA. Investigating whether genes in the flowering pathways are up-regulated in *AAF-OX* to contribute to the early flowering phenotype is of interest.

The expression of *AAF* is not restricted to senescent leaves but is also present in tissues where cells are highly proliferative (Fig. 1C, ii, iii, and viii); *AAF* may play a role in promoting growth by regulating local ROS levels. Several examples suggest ROS as signalling molecules instead of merely destructive by-products of cellular metabolism. For example, $O_2^{\cdot -}$ was found located in the apoplast of the cell elongation zone in roots, whereas H_2O_2 was accumulated in the differentiation zone and the cell wall of root hairs (Dunand *et al.*, 2007). Chemical treatments to reduce the local ROS levels affected root elongation and suppressed the formation of root hairs, which implies that ROS may function as signalling molecules to regulate root development (Dunand *et al.*, 2007). The *Arabidopsis rhd2* mutant has shorter roots and fewer root hairs than does the wild type, and the phenotype can be suppressed in part by exogenous ROS or is mimicked by chemical treatment to suppress ROS generation in roots (Foreman *et al.*, 2003). *RHD2* encodes an NADPH oxidase that can transfer electrons from NADPH to an electron acceptor to generate increased levels of ROS, so local ROS in roots is involved in cell outgrowth. In addition, localization and accumulation of ROS in roots can result from nutritional deprivation by nitrogen, phosphorus, and potassium deficiency that consequently modulates development of root hairs (Shin *et al.*, 2005). Levels of ROS were higher in the epidermis than in the cortex under potassium or nitrogen deprivation, whereas phosphorus deficiency resulted in ROS accumulation predominantly in the cortex of roots (Shin *et al.*, 2005). The pattern of patches of fluorescence in the roots of *AAF-OX* was similar to that seen with mineral deprivation. Moreover, the histochemical staining of *AAFpro::GUS* in the roots of seedlings indicated the tissue-specific expression of *AAF* in the elongation zone of primary and lateral roots (Fig. 1C, i and iii). The elongation of primary roots (Fig. 4C, D) and the formation of root hairs were enhanced in *AAF-OX* (Fig. 4E, F). Thus, *AAF* may be involved in development of root elongation and root hairs by modulating local ROS levels. However, *aaf-KO* did not show a delayed flowering phenotype or restricted root elongation and outgrowth of root hairs, which suggests that excessive cellular ROS (in *AAF-OX*) but not an elevated antioxidant capacity (in *aaf-KO*) plays a major role in flowering time and root development. Whether *AAF* is involved in the stress response to mineral deprivation remains to be explored.

AAF encodes a plastid protein in Arabidopsis and may be involved in redox homeostasis in chloroplasts

AAF is targeted to chloroplasts by transient expression of a GFP fusion protein in *Arabidopsis* mesophyll cells, and the putative transit peptide is required for plastid localization (Fig. 2). Intriguingly, despite a higher score in

predicted specificity than in AAF, SPA15 was localized to the cell wall in leaf tissues, as observed by immunogold electron microscopy (Supplementary Table S1 at *JXB* online) (Yap *et al.*, 2003). Both SPA15 and AAF have predicted transit peptides for targeting to plastids, but the subcellular localization results are not identical by two different assays. To clarify this discrepancy and verify the function of the predicted transit peptide in SPA15, a transient expression analysis was performed in *Arabidopsis* mesophyll protoplasts and it was found that SPA15–GFP was targeted to plastids (Supplementary Fig. S3). The results strongly support that the transit peptides in both AAF and SPA15 are *bona fide* plastid targeting signals in the protoplast transient assay.

A search of the plant genome database revealed that all of the AAF orthologues in different species are present as single loci (Supplementary Table S1). Phylogenetic analysis indicated AAF in the same clade as orthologues in monocots and moss, and with those in dicots in a different clade (Supplementary Fig. S2 at *JXB* online). The discovery of orthologues in moss suggests that the function of AAF may be present in the early evolution of land plants. The transgenic approach used here to elucidate the function of *AAF* provides a system to analyse the functional conservation of AAF orthologues from different species.

Chloroplasts are the major source of generating ROS in plants because of photosynthesis in an aerobic environment, and the oxidant scavenging systems and antioxidant networks are essential to remove excessive ROS to maintain redox homeostasis (Mittler, 2002; Foyer and Noctor, 2009). Paraquat perturbs the electron flow in PSI during photosynthesis and consequently induces accumulation of ROS to interfere with the redox poise in chloroplasts. Treatment with paraquat greatly enhanced the senescence-like phenotype and chlorophyll loss in *AAF-OX*, which was suppressed in *aaf-KO*, thus implying that *AAF* is probably involved in the redox balance in chloroplasts. Elevation of ROS levels in chloroplasts needs the recycling of oxidized antioxidants by enzymes such as SOD, ascorbate peroxidase (APX), monodehydroascorbate reductase (MDAR), dehydroascorbate reductase (DHAR), and glutathione reductase (GR) to remove excess ROS efficiently. In addition, NADPH generated by ferredoxin-NADP reductase (FNR) in PSI provides the reducing equivalents in the ascorbate–glutathione cycle, which produces the most abundant soluble antioxidants in plants. The increased levels of cellular ROS in *AAF-OX* may be due to lack of fully functional antioxidant enzymes for efficient reduction and recycling of oxidized antioxidants to remove ROS. It is possible that AAF negatively regulates the activity of one or several antioxidant enzymes to change the redox poise, whereas loss of *AAF* may contribute to an increased antioxidant capacity. Alternatively, overexpression of *AAF* may interfere with photosynthetic electron transport in chloroplasts to result in accumulation of ROS. Further analysis of the precise location of AAF in chloroplasts and identification of interacting proteins of AAF will provide more information to elucidate the physiological role of AAF in chloroplasts.

Despite the fact that the functional transit peptides at AAF and SPA15 for chloroplast localization were confirmed, the results did not exclude the possibility that both proteins may also localize to the cell wall in senescent leaves because of the nature of the transient protoplast experiment. ROS generated in apoplasts and chloroplasts result from biotic (pathogens) or abiotic (ozone, high light, and continuous darkness) stresses that may lead to leaf senescence and cell death. Because *AAF* is expressed in seedlings and in early senescent leaves and can be induced by ethylene and other stress hormones, it is possible that AAF is involved in response to developmental and stress signals to regulate redox homeostasis. On the basis of microarray data (Fig. 6, Table 1), it is possible that AAF is involved in response to oxidative stress, which may take place in chloroplasts as well as in apoplasts. Apoplastic ROS are involved in intra- and intercellular signalling and have a role in regulation of defence gene expression (Miller *et al.*, 2009). Furthermore, apoplastic ROS are not only involved in oxidative burst during pathogen infection, but also regulate cell growth (Gapper and Dolan, 2006; Sagi and Fluhr, 2006). ROS as signals to respond to plant development and stress depend on the ROS species, ROS intensity, and the site of production (Gechev *et al.*, 2006). Plasma membrane-bound NADPH oxidase and cell wall-associated peroxidase are the main enzymes to produce superoxide and H_2O_2 in the apoplast (Sagi and Fluhr, 2006). Localized superoxide generated by NADPH oxidase in the root hair tips triggers Ca^{2+} uptake essential for the root hair growth, which indicates that the site of ROS production is important (Foreman *et al.*, 2003). In addition, H_2O_2 can migrate across the membrane to act as a signal in activating the mitogen-activated protein kinase (MAPK) cascade to regulate downstream genes (Apel and Hirt, 2004). Whether AAF is involved in ROS homeostasis and/or response in apoplasts requires further research.

Hypersensitivity to oxidative stress and enhanced leaf senescence by overexpression of AAF depends on a functional EIN2

The mutant *ein2* shows enhanced resistance to oxidative stress as compared with the wild type (Alonso *et al.*, 1999; Cao *et al.*, 2006), which implies that the ethylene response is required to relay signals of induced ROS and the subsequent sensitivity to oxidative stress. By introducing the *ein2-5* allele in *AAF-OX*, it was shown that sensitivity to paraquat and H_2O_2 and dark-induced chlorophyll loss in *AAF-OX* was suppressed by *ein2-5*, which strongly supports that *EIN2* is epistatic to *AAF* and that a functional ethylene signalling pathway is required for *AAF* function. EIN2 has been shown to localize in the endoplamic reticulum (ER) membrane and interacts with the ethylene receptor ETR1 (Bisson *et al.*, 2009). The link of signal transduction from AAF in plastids to the ER-localized EIN2 to respond to oxidative stress and regulate leaf senescence remains to be established.

Phytohormones play differential roles in the onset, maintenance, and final stage of leaf senescence (Schippers *et al.*, 2007). The ethylene level is elevated at the onset of developmental leaf senescence, followed by the levels of JA, ABA, and finally SA that are increased to sustain the process of leaf senescence. Ethylene-insensitive mutants *etr1-1* and *ein2-1* showed delayed senescence and increased leaf longevity in *Arabidopsis* (Grbi'c and Bleecker, 1995; Oh *et al.*, 1997). Age-dependent leaf senescence was delayed in *AAF-OX*/*ein2-5* as in *ein2-5* (Chen and Wang, unpublished results). To understand the causal role of ethylene in AAF function, it was asked whether the expression of *AAF* is induced by ethylene. Indeed, it was found that ACC, the immediate precursor of ethylene, induced the expression of *AAF* by at least 2-fold and that the induction of *AAF* is dependent on a functional *EIN2*, suggesting that an ethylene response pathway is required to relay the signal (Fig. 9). However, *AAF* is not likely to be an immediate responsive gene, like *ERF1* (Fig. 9) (Solano *et al.*, 1998). Based on the essential role of a functional ethylene signalling pathway in *AAF* induction and in sensitivity to ROS, it is likely that there is a positive feedback regulation by ethylene to manifest *AAF* function during stress-induced and/or age-dependent leaf senescence. Yap *et al.* (2003) showed that *SPA15* transcript and protein in the detached leaves of sweet potato and rice were induced by ethylene as well as phytohormones involved in stress response and developmental senescence such as ABA, MeJA, and SA. The induction of *AAF* in light-grown seedlings by the same group of hormones was analysed in the present study. It was found that *AAF* expression was also induced by ABA, MeJA, and SA with different magnitudes and patterns (Supplementary Fig. S5 at *JXB* online). Both MeJA and SA induced *AAF* expression by ~2.5 fold, but the former showed an early induction at 6 h, and the latter at 2 d after treatment. Interestingly, *AAF* was induced by 4-fold at 6 h and gradually increased to 10-fold at 2 d after ABA treatment (Supplementary Fig. S5). These results indicate that the expression of *AAF* can be induced by all of the hormones tested, which is similar to previous observations for induction of *SAP15* in the leaves of sweet potato and rice (Yap *et al.*, 2003). Because ROS levels are affected by different stress responses and developmental senescence mediated by phytohormones such as ethylene, ABA, MeJA, and SA (Cho *et al.*, 2009), it is possible that *AAF* is involved in a common regulatory circuit to modulate redox homeostasis in various stress conditions. Further investigation of the mechanistic role of *AAF* in regulating cellular redox homeostasis will provide insights into the role of ROS in promoting leaf senescence and stress responses mediated by hormones.

Supplementary data

Supplementary data are available at *JXB* online.

Figure S1. Protein alignment of AAF orthologues.

Figure S2. Phylogenetic analysis of AAF orthologues.

Figure S3. SPA15 is targeted to chloroplasts in *Arabidopsis* mesophyll protoplasts.

Figure S4. Age-dependent leaf senescence and expression of *SAG12* and *SAG13* in 7-week-old *AAF-OX* and *aaf-KO* plants.

Figure S5. ABA, MeJA, and SA can induce *AAF* expression in light-grown *Arabidopsis* seedlings.

Table S1. Prediction of chloroplast targeting peptides of AAF orthologues by TargetP1.1.

Table S2. Primers used for genotyping, RT-PCR, and cloning.

Table S3. Primers used for quantitative PCR.

Acknowledgements

This work is dedicated to the late Professor Shu-Chen Grace Chen (1948–2007). We thank Dr Wann-Neng Jane and Mei-Jane Fang for technical assistance with electron microscopy and confocal laser microscopy; and Shu-Jen Chou and Min-Yan Kuo for technical support in the microarray experiments. We thank the ABRC and the Salk Institute for seeds of *aaf-KO* lines, and three anonymous reviewers for valuable comments. This work was supported partly by grants from the National Science Foundation to LCW (grant nos 94-2311-B-001, 97-2311-B-001) and by the Institute of Plant and Microbial Biology, Academia Sinica.

References

Agresti A. 1992. A survey of exact inference for contingency tables. *Statistical Science* **7,** 131–153.

Alonso JM, Hirayama T, Roman G, Nourizadeh S, Ecker JR. 1999. EIN2, a bifunctional transducer of ethylene and stress responses in Arabidopsis. *Science* **284,** 2148–2152.

Apel K, Hirt H. 2004. Reactive oxygen species: metabolism, oxidative stress, and signal transduction. *Annual Review of Plant Biology* **55,** 373–399.

Ashburner M, Ball CA, Blake JA, *et al*. 2000. Gene ontology: tool for the unification of biology. *Nature Genetics* **25,** 25–29.

Bisson MMA, Bleckmann A, Allekotte S, Groth G. 2009. EIN2, the central regulator of ethylene signalling, is localized at the ER membrane where it interacts with the ethylene receptor ETR1. *Biochemical Journal* **424,** 1–6.

Brychkova G, Alikulov Z, Fluhr R, Sagi M. 2008. A critical role for ureides in dark and senescence-induced purine remobilization is unmasked in the Atxdh1 Arabidopsis mutant. *The Plant Journal* **54,** 496–509.

Buchanan-Wollaston V. 1997. The molecular biology of leaf senescence. *Journal of Experimental Botany* **48,** 181–199.

Buchanan-Wollaston V, Earl S, Harrison E, Mathas E, Navabpour S, Page T, Pink D. 2003. The molecular analysis of leaf senescence—a genomics approach. *Plant Biotechnology Journal* **1,** 3–22.

Buchanan-Wollaston V, Page T, *et al*. 2005. Comparative transcriptome analysis reveals significant differences in gene expression and signalling pathways between developmental and dark/starvation-induced senescence in Arabidopsis. *The Plant Journal* **42,** 567–585.

Cao S, Jiang S, Zhang R. 2006. Evidence for a role of Ethylene-Insensitive 2 gene in the regulation of the oxidative stress response in Arabidopsis. *Acta Physiologiae Plantarum* **28,** 417–425.

Cho D, Shin D, Jeon B, Kwak J. 2009. ROS-mediated ABA signaling. *Journal of Plant Biology* **52,** 102–113.

Clough SJ, Bent AF. 1998. Floral dip: a simplified method for Agrobacterium-mediated transformation of Arabidopsis thaliana. *The Plant Journal* **16,** 735–743.

Dhindsa RS, Plumb-Dhindsa P, Thorpe TA. 1981. Leaf senescence: correlated with increased levels of membrane permeability and lipid peroxidation, and decreased levels of superoxide dismutase and catalase. *Journal of Experimental Botany* **32,** 93–101.

Dunand C, Crèvecoeur M, Penel C. 2007. Distribution of superoxide and hydrogen peroxide in Arabidopsis root and their influence on root development: possible interaction with peroxidases. *New Phytologist* **174,** 332–341.

Emanuelsson O, Nielsen H, Brunak S, von Heijne G. 2000. Predicting subcellular localization of proteins based on their N-terminal amino acid sequence. *Journal of Molecular Biology* **300,** 1005–1016.

Foreman J, Demidchik V, Bothwell JHF, *et al*. 2003. Reactive oxygen species produced by NADPH oxidase regulate plant cell growth. *Nature* **422,** 442–446.

Foyer CH, Noctor G. 2009. Redox regulation in photosynthetic organisms: signaling, acclimation, and practical implications. *Antioxidants and Redox Signaling* **11,** 861–905.

Gapper C, Dolan L. 2006. Control of plant development by reactive oxygen species. *Plant Physiology* **141,** 341–345.

Gechev TS, Van Breusegem F, Stone JM, Denev I, Laloi C. 2006. Reactive oxygen species as signals that modulate plant stress responses and programmed cell death. *BioEssays* **28,** 1091–1101.

Gepstein S, Sabehi G, Carp M-J, Hajouj T, Nesher MFO, Yariv I, Dor C, Bassani M. 2003. Large-scale identification of leaf senescence-associated genes. *The Plant Journal* **36,** 629–642.

Grbi'c V, Bleecker AB. 1995. Ethylene regulates the timing of leaf senescence in *Arabidopsis*. *The Plant Journal* **8,** 595–602.

He Y, Fukushige H, Hildebrand DF, Gan S. 2002. Evidence supporting a role of jasmonic acid in Arabidopsis leaf senescence. *Plant Physiology* **128,** 876–884.

He Y, Tang W, Swain JD, Green AL, Jack TP, Gan S. 2001. Networking senescence-regulating pathways by using Arabidopsis enhancer trap lines. *Plant Physiology* **126,** 707–716.

Huang Y-J, To K-Y, Yap M-N, Chiang W-J, Suen D-F, Chen S- CG. 2001. Cloning and characterization of leaf senescence up-regulated genes in sweet potato. *Physiologia Plantarum* **113,** 384–391.

Jing HC, Hebeler R, Oeljeklaus S, Sitek B, Stühler K, Meyer HE, Sturre MJG, Hille J, Warscheid B, Dijkwel PP. 2008. Early leaf senescence is associated with an altered cellular redox balance in Arabidopsis cpr5/old1 mutants. *Plant Biology* **10,** 85–98.

Jing HC, Sturre MJG, Hille J, Dijkwel PP. 2002. Arabidopsis onset of leaf death mutants identify a regulatory pathway controlling leaf senescence. *The Plant Journal* **32,** 51–63.

John CF, Morris K, Jordan BR, Thomas B, A-H-Mackerness S. 2001. Ultraviolet-B exposure leads to up-regulation of senescence-associated genes in Arabidopsis thaliana. *Journal of Experimental Botany* **52,** 1367–1373.

Kotchoni SO, Larrimore KE, Mukherjee M, Kempinski CF, Barth C. 2009. Alterations in the endogenous ascorbic acid content affect flowering time in Arabidopsis. *Plant Physiology* **149,** 803–815.

Kurepa J, Smalle J, Va M, Montagu N, Inzé D. 1998. Oxidative stress tolerance and longevity in Arabidopsis: the late-flowering mutant gigantea is tolerant to paraquat. *The Plant Journal* **14,** 759–764.

Lamb C, Dixon RA. 1997. The oxidative burst in plant disease resistance. *Annual Review of Plant Physiology and Plant Molecular Biology* **48,** 251–275.

Lim PO, Kim HJ, Nam HG. 2007. Leaf senescence. *Annual Review of Plant Biology* **58,** 115–136.

Lin J-F, Wu S- H. 2004. Molecular events in senescing *Arabidopsis* leaves. *The Plant Journal* **39,** 612–628.

Lohman KN, Gan S, John MC, Amasino RM. 1994. Molecular analysis of natural leaf senescence in Arabidopsis thaliana. *Physiologia Plantarum* **92,** 322–328.

Miller G, Schlauch K, Tam R, Cortes D, Torres MA, Shulaev V, Dangl JL, Mittler R. 2009. The plant NADPH oxidase RBOHD mediates rapid systemic signaling in response to diverse stimuli. *Science Signaling* 2, ra45.

Miller G, Shulaev V, Mittler R. 2008. Reactive oxygen signaling and abiotic stress. *Physiologia Plantarum* **133,** 481–489.

Miller G, Suzuki N, Ciftci-Yilmaz S, Mittler R. 2010. Reactive oxygen species homeostasis and signalling during drought and salinity stresses. *Plant, Cell and Environment* **33,** 453–467.

Miller JD, Arteca RN, Pell EJ. 1999. Senescence-associated gene expression during ozone-induced leaf senescence in Arabidopsis. *Plant Physiology* **120,** 1015–1024.

Mittler R. 2002. Oxidative stress, antioxidants and stress tolerance. *Trends in Plant Science* **7,** 405–410.

Mittler R, Vanderauwera S, Gollery M, Van Breusegem F. 2004. Reactive oxygen gene network of plants. *Trends in Plant Science* **9,** 490–498.

Morris K, Mackerness SAH, Page T, John CF, Murphy AM, Carr JP, Buchanan-Wollaston V. 2000. Salicylic acid has a role in regulating gene expression during leaf senescence. *The Plant Journal* **23,** 677–685.

Munné B, Alegre L. 2002. Plant aging increases oxidative stress in chloroplasts. *Planta* **214,** 608–615.

Murray MG, Thompson WF. 1980. Rapid isolation of high molecular weight plant DNA. *Nucleic Acids Research* **8,** 4321–4326.

Navabpour S, Morris K, Allen R, Harrison E, A-H-Mackerness S, Buchanan- Wollaston V. 2003. Expression of senescence-enhanced genes in response to oxidative stress. *Journal of Experimental Botany* **54,** 2285–2292.

Nielsen H, Engelbrecht J, Brunak S, von Heijne G. 1997. Identification of prokaryotic and eukaryotic signal peptides and prediction of their cleavage sites. *Protein Engineering* **10,** 1–6.

Oh SA, Park J-H, Lee GI, Paek KH, Park SK, Nam HG. 1997. Identification of three genetic loci controlling leaf senescence in Arabidopsis thaliana. *The Plant Journal* **12,** 527–535.

Orozco-Cardenas ML, Narvaez-Vasquez J, Ryan CA. 2001. Hydrogen peroxide acts as a second messenger for the induction of defense genes in tomato plants in response to wounding, systemin, and methyl jasmonate. *The Plant Cell* **13,** 179–191.

Procházková D, Wilhelmová N. 2007. Leaf senescence and activities of the antioxidant enzymes. *Biologia Plantarum* **51,** 401–406.

Rea G, de Pinto MC, Tavazza R, Biondi S, Gobbi V, Ferrante P, De Gara L, Federico R, Angelini R, Tavladoraki P. 2004. Ectopic expression of maize polyamine oxidase and pea copper amine oxidase in the cell wall of tobacco plants. *Plant Physiology* **134,** 1414–1426.

Sagi M, Fluhr R. 2006. Production of reactive oxygen species by plant NADPH oxidases. *Plant Physiology* **141,** 336–340.

Schippers JHM, Jing H-C, Hille J, Dijkwel PP. 2007. Developmental and hormonal control of leaf senescence. In: Gan S, ed. *Senescence processes in plants*. Oxford: Blackwell Publishing, 145–170.

Sheen J. 2001. Signal transduction in maize and Arabidopsis mesophyll protoplasts. *Plant Physiology* **127,** 1466–1475.

Shin R, Berg RH, Schachtman DP. 2005. Reactive oxygen species and root hairs in Arabidopsis root response to nitrogen, phosphorus and potassium deficiency. *Plant and Cell Physiology* **46,** 1350–1357.

Smart CM. 1994. Gene expression during leaf senescence. *New Phytologist* **126,** 419–448.

Solano R, Stepanova A, Chao Q, Ecker JR. 1998. Nuclear events in ethylene signaling: a transcriptional cascade mediated by ETHYLENE-INSENSITIVE3 and ETHYLENE-RESPONSE-FACTOR1. *Genes and Development.* **12,** 3703–3714.

Strother S. 1988. The role of free radicals in leaf senescence. *Gerontology* **34,** 151–156.

Weaver LM, Amasino RM. 2001. Senescence is induced in individually darkened Arabidopsis leaves, but inhibited in whole darkened plants. *Plant Physiology* **127,** 876–886.

Wintermans JF, de Mots A. 1965. Spectrophotometric characteristics of chlorophylls a and b and their pheophytins in ethanol. *Biochimica et Biophysica Acta* **109,** 448–453.

Woo HR, Kim JH, Nam HG, Lim PO. 2004. The delayed leaf senescence mutants of Arabidopsis, ore1, ore3, and ore9 are tolerant to oxidative stress. *Plant and Cell Physiology* **45,** 923–932.

Yap M-N, Lee R-H, Huang Y-J, Liao C- J, Grace Chen S-C. 2003. Molecular characterization of a novel senescence-associated gene SPA15 induced during leaf senescence in sweet potato. *Plant Molecular Biology* **51,** 471–481.